Journal of Crystal Growth 56 (1982) 189–205
North-Holland Publishing Company

GROWTH KINETICS OF ICE FROM THE VAPOUR PHASE AND ITS GROWTH FORMS

T. KURODA *
The Institute of Low Temperature Science, Hokkaido University, Sapporo 060, Japan

and

R. LACMANN
Institut für Physikalische Chemie der TU Braunschweig, Hans-Sommer-Strasse 10, D-3300 Braunschweig, Federal Republic Germany

Received 18 July 1981

A new interpretation of the habits of ice growing from vapour is proposed. The basic habits of ice alternate three times: plates (A) → −4°C → columns (B) → −10°C → plates (C) → between −20°C and −35°C → columns (D). The theory is based on a viewpoint that the surface of ice just below 0°C is covered with a quasi-liquid layer, whose thickness δ or coverage ϑ decreases with falling temperature, and therefore the growth mechanism of a crystal face changes also as follows: (I) Vapour–Quasi-Liquid–Solid mechanism ($\vartheta > 1$), (II) Adhesive Growth on a surface strongly adsorbed by H_2O molecules ($0.02 < \vartheta < 1$) and (III) Two-Dimensional Nucleation Growth on a surface with low eigen adsorption ($\vartheta < 0.02$). The type of surface structure and consequently the growth mechanism depends on the surface orientation and the temperature. The complicated habit change is caused mainly by the combination of surface kinetics of the $\{0001\}$ and $\{10\bar{1}0\}$ face. The first and second conversion temperature (T_{AB}, T_{BC}) are expected to be independent of the absolute supersaturation ΔP as found in experiments. On the other hand, the third (T_{CD}) is the temperature where the usual two-dimensional nucleation growth rate of the $\{0001\}$ face reaches the one of the $\{10\bar{1}0\}$ face, and exceeds it by the effect of diffusion field, so that the third conversion temperature falls with decreasing ΔP. The marked columnar crystals observed at −7°C can be explained only by taking into account the spherical volume diffusion field near the $\{0001\}$ face and a cylindrical one near the $\{10\bar{1}0\}$ face. For plate-like crystals between −10°C and −20°C to −35°C the surface diffusion from $\{0001\}$ to $\{10\bar{1}0\}$ and volume diffision with cylindrical symmetry near $\{10\bar{1}0\}$ faces is very important.

1. Introduction

The ice crystals grown from the vapour phase, i.e. snow crystals, have attracted us for a long time because of the variety in their beautiful forms. In 1938 Nakaya and his co-workers [1] succeeded in growing artificial ice crystals in a convective air stream so as to investigate the relation between growth forms and experimental conditions. Since these early beginnings, much experimental research on growth forms of snow crystals has been done by Nakaya's school [2,3], Aufm Kampe, Weickmann and Kelly [4], Mason [5], Kabayashi [6,7], Hallett and Mason [8], and others. These results have been consolidated in the Kobayashi diagram [7] (fig. 1).

The diagram shows that three conversions occur in the basic form or habit at $T_{AB} = -4°C$ (plates (A) to columns (B)), $T_{BC} = -10°C$ (columns (B) to plates (C)), and $T_{CD} = -22°C$ (plates (C) to columns (D)). The first and the second conversion at T_{AB} and T_{BC} occur within temperature intervals of less than 1 K [7], while the third one at T_{CD} is much less sharp [9]. Recently, hexagonal plates have been observed at temperatures below −30°C and low supersaturation [10–12]. Gonda [12] reported that small single crystals (<30 μm) grown in free fall in helium and argon gases at −30°C and about 4% supersaturation, and at −44°C near ice saturation were almost plates. Anderson et al. [11] have found that at −30°C the

* The paper is based on the author's Dr.rer.nat. thesis, TU Braunschweig, 1979.

0022-0248/82/0000–0000/$02.75

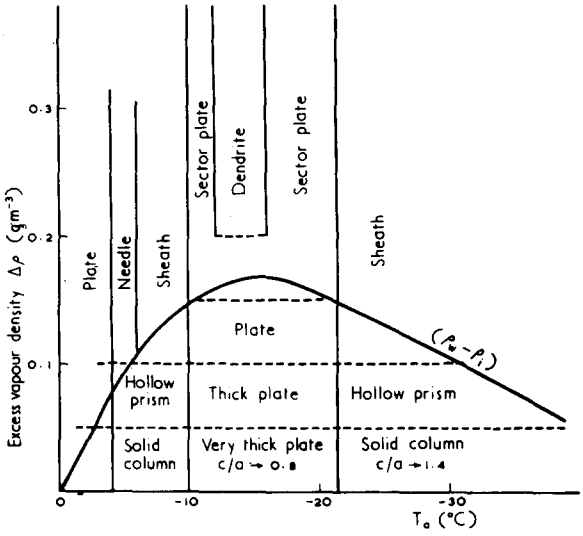

Fig. 1. Growth forms of ice crystal from the vapour depending on temperature and absolute supersaturation ΔP (Torr) = $T\Delta\rho(g/m^3)/288$ (Kobayashi [7]).

habit of ice crystals changes from plates to columns with supersaturation exceeding 25% (over ice). These results imply that the third conversion temperature T_{CD} from plates to columns depends on supersaturation. The change in basic habits mentioned above has not been explained theoretically. The Kobayashi diagram shows also that the type of growth (e.g., polyhedral growth, dendritic growth, and so on) depends on supersaturation. Frank [13] suggested that the dendritic growth of snow crystals is due first to the preferred growth by two-dimensional nucleation at corners where the supersaturation is larger and second to the lacunary (skeletal) growth towards the facet centre. Frank also discussed qualitatively the formation of three-dimensional structure of external forms of snow crystals. The same problems of morphological instability of the singular interface due to the inhomogeneity in supersaturation along the interface were pursued quantitatively in case of solution growth by Chernov [14], and Kuroda, Irisawa and Ookawa [15]. Lacmann and Stranski [16] interpreted the direction of the dendrites of snow crystals using a quasi-liquid layer model.

Yamashita [17] measured the temperature dependence of the length of the c and a axes of falling ice crystals 200 s after seeding at water saturation in a large cloud chamber (fig. 2). Similar experiments were carried out by Ryan et al. [18].

The relative supersaturation against ice at water saturation

$$\Delta P/P_I = (P_W - P_I)/P_I$$

increases with decreasing temperature, while the absolute supersaturation $\Delta P = P_W - P_I$ goes through a maximum (fig. 3). Here P_W and P_I are the equilibrium vapour pressure of water and ice respectively.

Anderson et al. [11] have observed the supersaturation dependence of the growth of ice crystals on covellite and silver iodide single crystals within the temperature range from −10 to −22°C. A number of crystals failed to grow at all in the c axis direction at vapour pressures between ice and water saturation, although they grew laterally. As the supersaturation increased, however, the growth in the c axis began. The results suggest that the {0001} faces at temperatures between −10 and −22°C grow by two-dimensional nucleation without the aid of screw dislocations. McKnight and Hallett [19] using X-ray topography have actually confirmed that the plate like ice crystals were often free from dislocations.

Keller et al. [20] have recently stated the transition from plates to columns between −4 and −8°C with increasing supersaturation. It is, however, rather difficult to determine the actual growth conditions in their experiments, since too many ice crystals grow on a fibre cooled by liquid nitrogen.

Isono et al. [21] were the first to point out the importance of the vapour diffusivity and thermal conductivity for the growth forms of ice crystals. Then Gonda and Komabayashi [22], and Gonda [23] investigated the effect of the vapour diffusivity and thermal conductivity on the growth of ice crystals falling in helium–argon gas mixtures. The results with regard to the effect of vapour diffusivity at constant thermal conductivity are as follows (see fig. 4):
(a) As the diffusion coefficient of water vapour increases at −15°C, the growth rate R and the ratio of axes c/a increases and c/a approaches unity. At the same time, the hexagonal plates with extending branches vary to hexagonal plates with skeletal structures without branches, which vary to solid hexagonal plates without skeletal structures and branches.
(b) As the diffusion coefficient increases at −7°C, R increases and c/a decreases to unity. Columns with

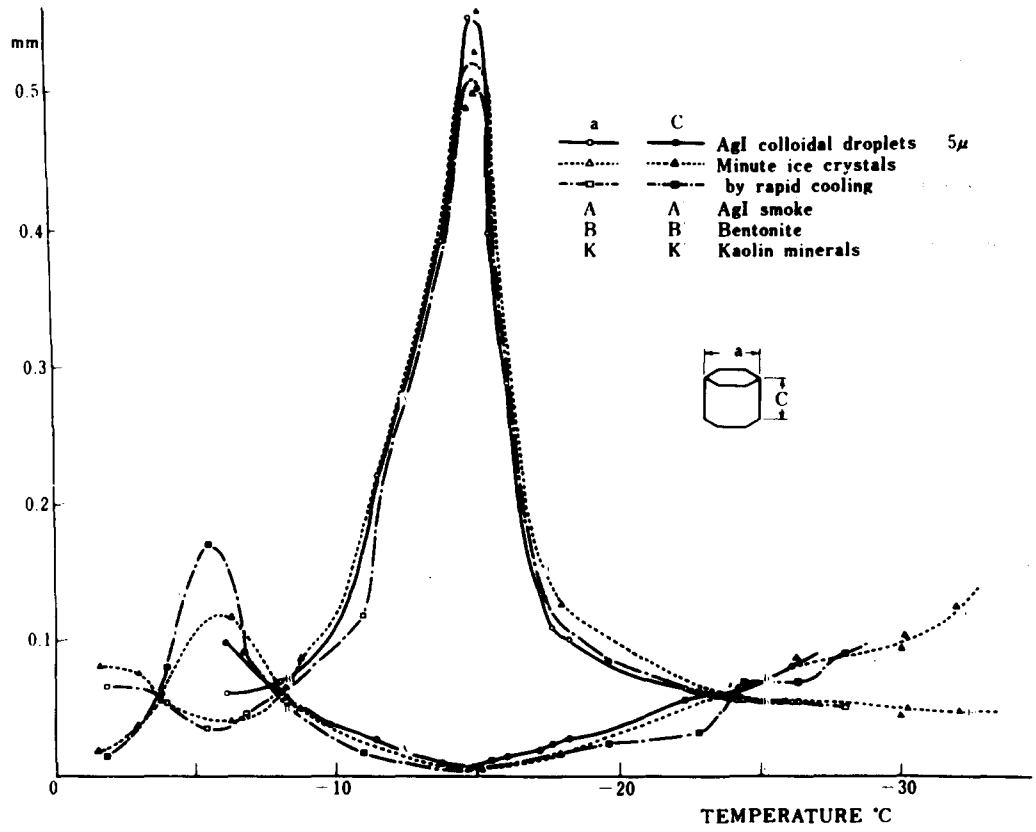

Fig. 2. Temperature dependence of the length of *c* and *a* axis 200 s after seeding (Yamashita [17]).

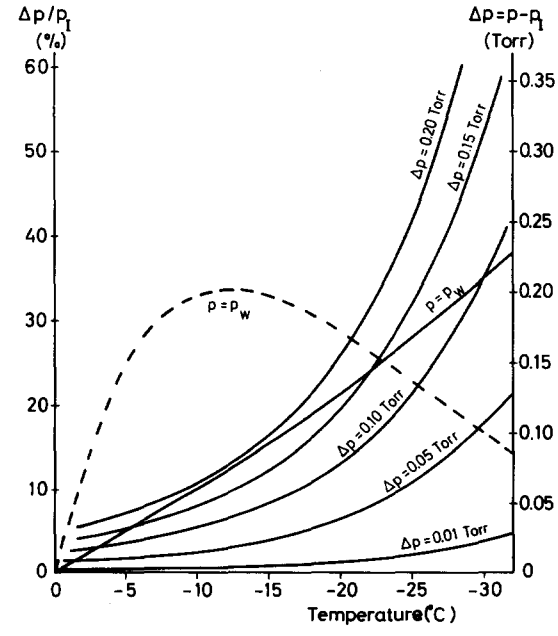

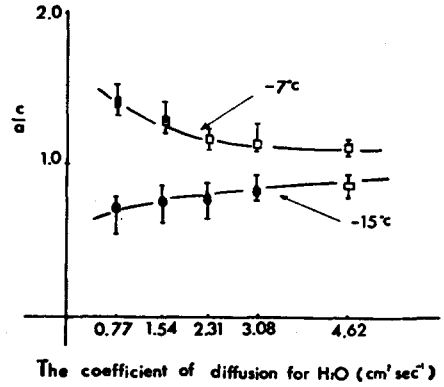

Fig. 4. The ratio *c*/*a* as a function of the diffusion coefficient at constant thermal conductivity (Gonda and Komabayashi [22]).

Fig. 3. Relative supersaturation $\Delta P/P_I(\%)$ (———) at constant ΔP and at water saturation, and the absolute supersaturation ΔP(Torr) (– – –) at water saturation as a function of temperature.

hollows change to solid columns without skeletal structures. These results suggest that the diffusion field of water vapour surrounding a ice crystal contributes to the formation of the marked form.

To investigate the growth mechanism, Hallett [24] and Kobayshi [25] measured the temperature dependence of the velocity of giant steps on the {0001} face. Both found a remarkable trend which contains a maximum of the velocity. Mason et al. [9] measured the interaction distance between giant steps as a function of temperature and made it identical to twice the mean migration distance $\bar{x}_s$ of the adsorbed molecules. The variations of $\bar{x}_s$ were similar to the change in the velocity v of a giant step. The trends with temperature of $\bar{x}_s$ and v have not been explained.

Lamb and Hobbs [26], and Lamb and Scott [27] measured the growth rate of the basal and prism faces of ice crystals on a stainless steel substrate in a vacuum chamber as a function of temperature T at $\Delta P = 0.01$ Torr. This supersaturation corresponds to a relative supersaturation $\Delta P/P_I < 1\%$ in the investigated temperature range ($T > -17°C$). The relation between $R(0001)$ and $R(10\bar{1}0)$ was compatible with the alternation with temperature of the basic habits.

It should be noticed that the observed growth rates just below 0°C are extraordinally large in comparison to other crystals growing from the vapour phase at such a small relative supersaturation (see table 1). This means that there must be something on the ice surface near the melting point that promotes the growth. In sections 2 and 3 it will become clear that a quasi-liquid layer on the ice surface contributes to the promotion of the growth of the ice crystal just below 0°C.

The properties of the ice surface have attracted scientific interest for more than a century. In order to explain the many peculiar mechanical properties of ice like regelation, Faraday [33] postulated that at temperatures not too far below the melting point the surface of ice is covered with a thin film of water. Weyl [34] revived these ideas and gave qualitative arguments for its existence. Fletcher [35] investigated the stability of a quasi-liquid layer from statistical and thermodynamical considerations and discussed the variation of the layer thickness with temperature. On the other hand, various indirect measurements have indicated the existence of a quasi-

Table 1
The growth rates of various substances from the vapour phase

Substance	T (°C)	P_{eq} (Torr)	$\Delta P/P_{eq}$	R (μm/s)	Author
Ice ($10\bar{1}0$)	−5	3.01	3.3×10^{-3}	5×10^{-1}	Lamb and Scott (1972) [27]
Iodine	0	3.7×10^{-2}	1.0×10^{-2}	9×10^{-3}	Volmer and Schultze (1931) [28]
	25	3.4×10^{-1}	1.0×10^{-2}	1.4×10^{-2}	Bradley and Drury (1959) [29]
CBr_4 (mon)	40	2.04	1.0×10^{-2}	1.1×10^{-1}	Bradley and Drury (1959) [29]
CBr_4 (cub)	50	3.86	1.0×10^{-2}	7×10^{-3}	
Hexmethylentetramine (011) ($C_6H_{12}N_4$)	70	3.4×10^{-2}	8.0×10^{-3}	5×10^{-4}	Honigmann and Heyer (1956) [30]
Zinc	394	6.8×10^{-2}	1.0×10^{-2}	8×10^{-4}	Parker and Kushner (1961) [31]
Benzophenone (110) ($C_{13}H_{10}O$)	25	6.1×10^{-4}	6.0×10^{-2}	1×10^{-3}	Kitchner and Stickland-Constable (1958) [32]
Sulphur	60	6.3×10^{-4}	1.0×10^{-2}	5×10^{-4}	Kitchner and Stickland-Constable (1958) [32]

liquid layer on the ice surface just below 0°C. These include mechanical [36–41], electrical [42–45], gas adsorption [46,47], and especially NMR studies [48, 49], and more recently photo emission [50], Volta effect [51], proton channeling [52], thermal expansion [53] and ellipsometry [54] measurements.

In contrast to much experimental research on growth forms of ice crystals from the vapour phase, there are few theoretical works. There is no satisfactory explanation for the variation of basic forms with temperature and supersaturation, even though several attempts have been made by Mason et al. [9], Lamb and Scott [55], and Lacmann [56].

In this paper a new interpretation of the change in basic forms of ice crystals is proposed. Since the basic form, i.e. plates ($c/a < 1$) or columns ($c/a > 1$), is determined by the ratio of the growth rates of basal {0001} and prism {10$\bar{1}$0} faces, we must consider the variation of the surface structure of ice crystals as well as surface kinetics of growth with temperature and surface orientation in order to pursue the problem. Then, the effects of diffusion field of water vapour to the growth forms are also discussed.

2. Thermodynamics of a quasi-liquid layer

At present the hypothesis of a quasi-liquid layer on the ice surface is accepted on the basis of several pieces of experimental evidences [36–54] as mentioned in section 1. It is agreed, that the layer is stable above about -20 ± 10°C. Fletcher [35] has shown the stability of the quasi-liquid layer theoretically. However, these experimental and theoretical works have not considered the orientation dependence of the equilibrium layer thickness even though it is very important for the study of the growth of ice crystals as well as their basic habits. Lacmann and Stranski [16] proposed a phenomenological model of quasi-liquid layer based on a macroscopic concept of wettability $\Delta\sigma_\infty$, in order to investigate the orientation of dendrites of snow crystals. Lacmann [56] also discussed the basic habits of ice crystals at temperatures between 0 and -10°C using the model. This model is suitable for our purpose, because the orientation dependence of the layer thickness is taken into consideration through the wettability $\Delta\sigma_\infty$. We shall proceed to the subject using the developed Lacmann–Stranski model [16,57].

2.1. Equilibrium thickness of a quasi-liquid layer

The existence of a quasi-liquid layer below the melting temperature is disadvantageous in the sense of bulk free energy of the liquid phase. The quasi-liquid layer can exist just below 0°C, because it lowers the surface free energy of the system. The wettability parameter $\Delta\sigma_\infty$ defined by the following equation is positive for the ice/water system as shown in section 3:

$$\Delta\sigma_\infty = \sigma_I - (\sigma_W + \sigma_{I/W}) > 0. \tag{2.1}$$

Here σ_I is the surface tension of ice without a quasi-liquid layer, σ_W that of water and $\sigma_{I/W}$ the interfacial tension between ice and water.

Fig. 5 shows the total free energy Δf of the system as a function of the thickness δ of the quasi-liquid layer given by [16,57]:

$$\Delta f(\delta) = \sigma_W + \sigma_{I/W} + \frac{A^n}{(A+\delta)^n}\Delta\sigma_\infty + \frac{\delta}{V_m} kT \ln\frac{P_W}{P_I}. \tag{2.2}$$

There is equilibrium between ice and quasi-liquid layer at the minimum of Δf ($\delta = \delta_{eq}$). The equilibrium thickness δ_{eq} is given by

$$\delta_{eq} = -A + \left[\frac{nA^n \Delta\sigma_\infty V_m}{kT \ln(P_W/P_I)}\right]^{1/(n+1)} = -A + \left[\frac{nA^n \Delta\sigma_\infty V_m T_m}{Q_m \Delta T}\right]^{1/(n+1)}, \tag{2.3}$$

if we use

$$\Delta\mu_{I/W} = kT \ln(P_W/P_I) \approx (Q_m/T_m)\Delta T.$$

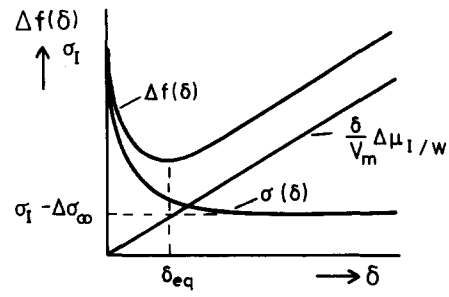

Fig. 5. Total free energy of a quasi-liquid layer as a function of the thickness δ.

Here T_m is the melting temperature of ice (T_m = 273.15 K or 0°C), Q_m the molecular heat of melting of ice, V_m the molecular volume of water in the quasi liquid layer and $\Delta T = T_m - T$ the supercooling. A and n are the parameters which should be determind by the microscopic theory or future experiments. In the paper of Lacmann and Stranski [16] and Lacmann [56], $n = 1$ and A is the parameter of the radius of action of the intermolecular forces. According to the rough estimation using Van der Waals interaction [57], A is a radius of a molecule and $n = 2$. Ruckenstein [58] has discussed the free energy of a thin film as a function of its thickness using Lennard-Jones potentials, in order to study the sintering mechanism of metal crystallites on a substrate. The dependence on temperature and surface orientation of δ_{eq} is discussed in section 3.

2.2. *Equilibrium vapour pressure and chemical potential of a quasi-liquid layer as a function of* δ

We have obtained the equilibrium vapour pressure $P(\delta)$ or the adsorption isotherm of a quasi-liquid layer as follows [16,57]:

$$\ln \frac{P(\delta)}{P_W} = -\frac{nA^n \Delta\sigma_\infty V_m}{kT(A+\delta)^{n+1}} . \qquad (2.4)$$

$P(\delta)$ increases with δ, $P(\delta) = P_W$ at $\delta = \infty$, and $P(\delta) = P_I$ at $\delta = \delta_{eq}$ (fig. 6).

The chemical potential of the quasi-liquid layer referred to that of ice is given by

$$\Delta\mu(\delta) = kT \ln(P(\delta)/P_I) .$$

$\Delta\mu(\delta)$ increases with δ, $\Delta\mu(\delta) = 0$ at $\delta = \delta_{eq}$, $\Delta\mu(\delta) = \Delta\mu_{I/W} = kT \ln(P_W/P_I)$ (chemical potential of the undercooled water) at $\delta = \infty$, and $\Delta\mu(\delta) < 0$ if $\delta < \delta_{eq}$ (fig. 7).

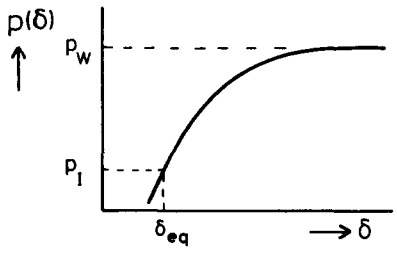

Fig. 6. The equilibrium vapour pressure $P(\delta)$ of a quasi-liquid layer as a function of δ.

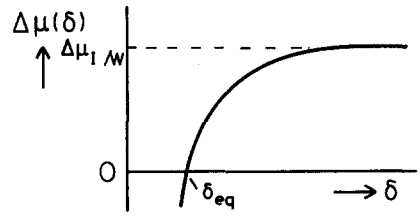

Fig. 7. The chemical potential $\Delta\mu(\delta)$ of a quasi-liquid layer as a function of δ.

3. Change of surface structure of ice crystals with temperature and its dependence on the crystal orientation

The equilibrium thickness δ_{eq} is infinite at the melting temperature and decreases with falling temperature, because the disadvantage of the free energy of bulk liquid increases with decreasing temperature (fig. 8). δ_{eq} becomes equal to the thickness of a monolayer (≈3 Å) at a certain temperature $T_{I/II}$. The coverage ϑ of the surface by water molecules is equal unity at $T_{I/II}$. Therefore, the model of a quasi-liquid layer is valid only for the temperatures $T_m > T >$

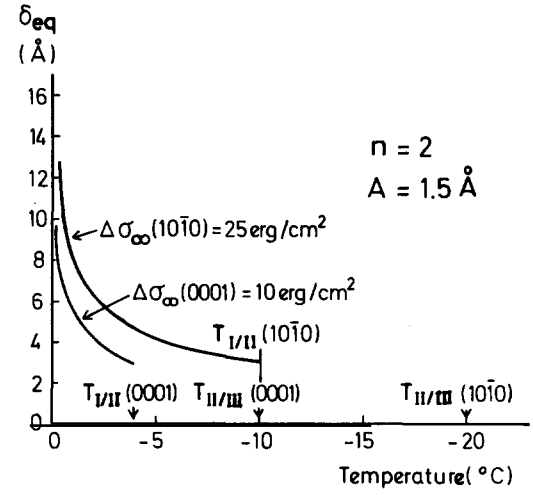

Fig. 8. The equilibrium thickness δ_{eq} of a quasi-liquid layer depending on temperature and surface orientation.

$T_{I/II}$. However, a layer thickness less than a monolayer at temperatures below $T_{I/II}$ corresponds to a surface strongly adsorbed by H_2O molecules with a coverage $\vartheta < 1$. This surface may be uneven or rough on a molecular level. The number of adsorbed molecules decreases with falling temperature and becomes very small, e.g. $\vartheta < 0.02$, at a certain temperature $T_{II/III}$. The surface at temperatures below $T_{II/III}$ is expected to be the singular one with little eigenadsorption ($\vartheta < 0.02$), as the usual solid/vapour interface of other crystals. Fig. 9 shows schematically the change of the surface structure of the referred surface as a function of temperature.

We next discuss the dependence of δ_{eq} on crystal orientation. δ_{eq} increases with $\Delta\sigma_\infty$, and $\Delta\sigma_\infty$ depends on crystal orientation through σ_I and $\sigma_{I/W}$ in eq. (2.1). According to a rough estimation using the number of the broken bonds at the surface and the heat of sublimation $Q_{sub} = 676$ cal/g or 8.5×10^{-13} erg/molecule,

$$\sigma_I(0001) = 121 \quad \text{and} \quad \sigma_I(10\bar{1}0) = 128 \text{ erg/cm}^2 .$$

If we assume that $\sigma_{I/W}$ is proportional to σ_I, and the proportion is equal to the ratio of heat of fusion ($Q_m = 80$ cal/g or 1.0×10^{-13} erg/molecule) and heat of sublimation (Q_{sub}), we get

$$\sigma_{I/W}(0001) = 14 \quad \text{and} \quad \sigma_{I/W}(10\bar{1}0) = 15 \text{ erg/cm}^2 .$$

The experimental value [59] for $\sigma_{I/W}$ measured by observation of the equilibrium shape of grain boundary grooves at the water/ice interface is 29.1 ± 0.8 erg/cm^2. On the other hand, the experimental value for σ_W at 0°C is 78 erg/cm^2. From these values, we obtain

$$\Delta\sigma_\infty(0001) = 31 \quad \text{and} \quad \Delta\sigma_\infty(10\bar{1}0) = 37 \text{ erg/cm}^2 .$$

Because of the rough estimation, the absolute values of $\Delta\sigma_\infty$ are not accurate, but it is sure that the $\{10\bar{1}0\}$ face has a larger wettability than the $\{0001\}$ face which has smaller σ_I, i.e. $\Delta\sigma_\infty(10\bar{1}0) > \Delta\sigma_\infty(0001)$.

To draw fig. 8, the following numerical values are used: $\Delta\sigma_\infty(0001) = 10$, $\Delta\sigma_\infty(10\bar{1}0) = 25$ erg/cm^2, $n = 2$ and $A = 1.5$ Å. Therefore the quasi-liquid layer on the $\{10\bar{1}0\}$ face which has a larger $\Delta\sigma_\infty$ is thicker than that on the $\{0001\}$ face at the same temperature, and remains thicker than 3 Å until lower temperature; i.e. (fig. 8):

$$T_{I/II}(10\bar{1}0) < T_{I/II}(0001).$$

The transition temperature $T_{II/III}$ from the surface with strong eigenadsorption to that with little eigenadsorption is also expected to be lower for prism faces than for basal faces (fig. 8):

$$T_{II/III}(10\bar{1}0) < T_{II/III}(0001).$$

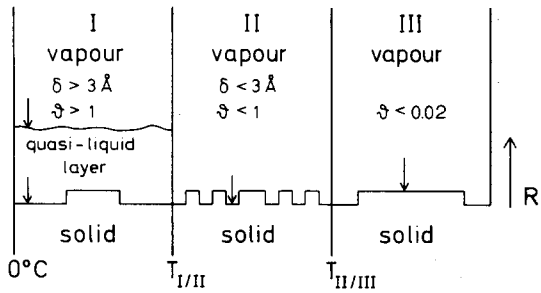

Fig. 9. Variation of surface structure and surface kinetics of growth with temperature: (I) V–QL–S mechanism; (II) adhesive growth; (III) the usual two-dimensional nucleation growth.

4. Growth kinetics of ice from the vapour phase

4.1. Surface kinetics

As shown in section 3, the structure of a surface of ice changes twice with falling temperature; the surface covered with a quasi-liquid layer ($\vartheta > 1$) changes to a surface with strong eigenadsorption by water molecules ($1 > \vartheta > 0.02$) at $T_{I/II}$. The latter surface becomes a singular one with low eigenadsorption ($\vartheta < 0.02$) at $T_{II/III}$. Therefore, the surfaces grow by three distinctive growth mechanism as follows:

(I) Vapour–Quasi-Liquid–Solid mechanism ($0°C > T > T_{I/II}$; $\vartheta > 1$)

(II) Adhesive Growth on a surface with strong adsorption by water molecules ($T_{I/II} > T > T_{II/III}$; $1 > \vartheta > 0.02$), and

(III) Two-Dimensional Nucleation Growth on a singular surface with low eigenadsorption ($T < T_{II/III}$; $\vartheta < 0.02$).

The three mechanisms are discussed in detail below.

(I) V–QL–S mechanism ($0°C > T > T_{I/II}$; $\vartheta > 1$). The growth of ice crystals covered with a quasi-liquid layer consists of two phase transitions. At first, the condensation of water vapour into the quasi-liquid layer occurs with the rate R_{Ia}, and then ice grows with the rate R_{Ib} at the quasi-liquid/ice interface [16] (fig. 9).

The condensation rate R_{Ia} is given by the Hertz–Knudsen equation:

$$R_{Ia} = \alpha[P - P(\delta)]V_m/(2\pi mkT)^{1/2}\,, \tag{4.1}$$

where P is the actual pressure of water vapour, $P(\delta)$ the equilibrium vapour pressure of a quasi-liquid layer given by eq. (2.4), and α the condensation coefficient. Using a pressure jump relaxation method, Schulze and Cammenga [60] have shown that $\alpha = 1$ for water at 20°C. R_{Ia} is a decreasing function of δ, because $P(\delta)$ increases with δ (fig. 6).

The expression for the crystallization rate R_{Ib} is obtained from the analogy of ice growth from the melt, i.e. water ($\delta = \infty$). Since the perfection of crystals growing from the vapour phase is usually good, R_{Ib} is determined by two-dimensional nucleation at the quasi-liquid/ice interface. Then, under certain assumptions $R_{Ib}(\delta)$ is given by

$$R_{Ib}(\delta) = C\exp(-\Delta G^*_{2ql}/3kT)\,, \tag{4.2}$$

with

$$\Delta G^*_{2ql} = \pi\gamma^2_{ql} f_0/\Delta\mu(\delta)\,, \tag{4.2'}$$

$$C = l(2\pi/3)^{1/3}\{\Delta\mu(\delta)/kT\}^{5/6}\,\nu\exp(-E_d/kT)\,. \tag{4.2''}$$

Here ΔG^*_{2ql} is the formation free energy of the two-dimensional nucleus, γ_{ql} the edge free energy of the nucles, f_0 the occupied area by a molecule, l the average jump distance, ν the frequency factor, and E_d the activation free energy for diffusion in a quasi-liquid layer. The factor 1/3 in the exponent of the equation (4.2) characterizes the polynucleation growth (Hillig [61]), which is proportional to the cubic root of the nucleation rate. $R_{Ib}(\delta)$ increases with $\Delta\mu(\delta)$ or δ at constant temperature (fig. 10). $R_{Ib}(\delta_{eq}) = 0$ since the quasi-liquid layer exists in equilibrium with ice ($\Delta\mu(\delta_{eq}) = 0$). $R_{Ib}(\infty)$ agrees with the crystallization rate from the melt (Hillig [62]). At steady state both rates R_{Ia} and R_{Ib} must be equal:

$$R_{Ia}(\delta_{st}(T), P) = R_{Ib}(\delta_{st}(T)) = R_I(T, \Delta P). \tag{4.3}$$

From this balance equation, we can calculate the thickness $\delta_{st}(T, P)$ of a quasi-liquid layer and the growth rate $R_I(T, \Delta P)$ under steady state conditions as a function of temperature T and absolute supersaturation ΔP (fig. 10).

According to experiments by Hillig [62], the crystallization rate of the ice {0001} face is proportional to $\exp(-0.35/\Delta T)$. The value for $\gamma_{ql}(0001)$ estimated from this result is 7.22×10^{-8} erg/cm (corresponding to 2.15×10^{-15} erg/molecule). The value is much smaller than that of the vapour/ice surface with low eigenadsorption ($T < T_{II/III}$; $\vartheta < 0.02$). Namely, the quasi-liquid layer promotes the growth of ice from the vapour at lower supersaturation in comparison with the growth of other crystals (table 1).

(II) Adhesive growth on a surface with strong eigenadsorption ($T_{I/II} > T > T_{II/III}$; $1 > \vartheta > 0.02$). As the surface strongly adsorbed by H_2O molecules is rough on a molecular level, the incoming molecules from the vapour can be easily incorporated into the crystal (fig. 9). If no other process except surface kinetics is involved, the rate R_{II} of the adhesive growth is given by the Hertz–Knudsen equation with $\alpha = 1$:

$$R_{II} = (P - P_I)\,V_m/(2\pi mkT)^{1/2}. \tag{4.4}$$

R_{II} is the maximum growth rate R_{max} from the vapour at a certain supersaturation.

According to the Monte-Carlo simulation by De Hahn et al. [63], the surface kinetics of growth is distinguished by the equilibrium concentration of an adunit, i.e. coverage ϑ. Roughly speaking, adhesive growth takes place on the surface with $\vartheta > 0.02$, while two-dimensional nucleation growth occurs on the surface with $\vartheta < 0.02$.

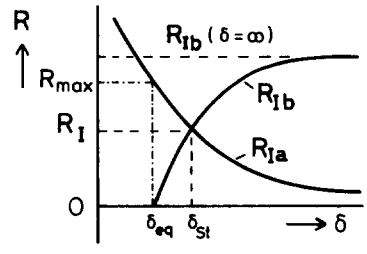

Fig. 10. R_{Ia} and R_{Ib} as a function of δ.

(III) Two-dimensional nucleation growth on a surface with low eigenadsorption ($T < T_{II/III}$; $\vartheta <$ 0.02). The growth of a singular surface with low eigenadsorption (<0.02) is determined by the two-dimensional nucleation mechanism (fig. 9). The rate of polynucleation growth R_{III} is determined by the nucleation rate J as well as the step velocity v. If the step distance is larger than twice the mean surface diffusion distance $\bar{x}_s$ of admolecules under certain additions R_{III} is given by

$$R_{III} = dJ^{1/3}v^{2/3} \tag{4.5}$$

with

$$J = \frac{P^2}{2\pi mkT}\,\bar{x}_s^2\left(\frac{\Delta\mu_{I/V}}{kT}\right)^{1/2}\frac{1}{\nu} \times \exp\left(\frac{E_a}{kT}\right)\exp\left(-\frac{\Delta G^*_{2V}}{kT}\right), \tag{4.6}$$

$$v = 2\bar{x}_s f_0\,\frac{(P - P_I)}{(2\pi mkT)^{1/2}}, \tag{4.7}$$

$$\bar{x}_s = l\exp[(E_{ad} - E_{sd})/2kT]\,. \tag{4.8}$$

Here ΔG^*_{2V} is the formation free energy of the two-dimensional nucleus depending on the relative supersaturation $\Delta P/P_I$ and the edge free energy γ_V, $\Delta\mu_{I/V}$ the chemical potential of the vapour phase against ice, E_{ad} the adsorption energy and E_{sd} the activation energy for surface diffusion. If we assume that a two-dimensional nucleus on the {0001} face is of regular hexagonal shape and that the one on the $\{10\bar{1}0\}$ face is rectangular as determined by Wulff's theorem [57], we obtain the formation free energy of the two-dimensional nuclei:

$$\Delta G^*_{2V}(0001) = \frac{6[\gamma_V(0001)]^2 f_0(0001)}{\sqrt{3}\,\Delta\mu_{I/V}}, \tag{4.9}$$

$$\Delta G^*_{2V}(10\bar{1}0) = \frac{4[\overline{\gamma_V(10\bar{1}0)}]^2 f_0(10\bar{1}0)}{\Delta\mu_{I/V}}, \tag{4.10}$$

where

$$\Delta\mu_{I/V} = kT\ln(P/P_I) \approx kT\,\Delta P/P_I\,.$$

The edge free energy of the two-dimensional nucleus is obtained by the Stranski–Kaischew method [57, 64]:

$$\gamma_V(0001) = \varphi_1/2a_0\,, \tag{4.11}$$

$$\overline{\gamma_V(10\bar{1}0)} = \varphi_1/2(a_0c_0)^{1/2}\,, \tag{4.12}$$

where φ_1 is the binding energy between nearest neighbours, a_0 the molecular distance in $[2\bar{1}\bar{1}0]$ direction (4.52 Å) and c_0 the height of the unit cell in the c axis (7.36 Å). The area occupied by a molecule f_0 is:

$$f_0(0001) = \sqrt{3}\,a_0^2/4 \tag{4.13}$$

$$f_0(10\bar{1}0) = a_0c_0/4. \tag{4.14}$$

Using eqs. (4.9) to (4.14), the relations

$$\gamma_V(0001) > \overline{\gamma_V(10\bar{1}0)},$$

$$\Delta G^*_{2V}(0001) > \Delta G^*_{2V}(10\bar{1}0),$$

are valid. This means that nucleation takes place more easily on $\{10\bar{1}0\}$ faces than on {0001} faces. This result is valid also for the V–QL–S mechanism.

Since φ_1 is half the heat of sublimation (Q_{sub} = 8.5×10^{-13} erg/molecule), $\varphi_1 = 4.25 \times 10^{-13}$ erg/molecule, $\gamma_V(0001) = 4.7 \times 10^{-6}$ erg/cm and $\overline{\gamma_V(10\bar{1}0)} = 3.7 \times 10^{-6}$ erg/cm.

4.2. Diffusion process of water vapour

In section 4.1 we discussed how the growth rate is determined by the three types of surface kinetics. If the growth rate is very large and water molecules are easily incorporated into the crystal, we must take into account the diffusion of water vapour in air or other gases. This diffusion process is very important for the interpretation of the marked forms ($c/a \ll 1$ or $c/a \gg 1$) of ice crystals and appearance of columnar crystals at temperatures below –20°C.

Neglecting convection effects, one can write for the growth rate by diffusion R_D of a spherical crystal with radius r_{cr} in a spherical vessel with radius r_{ve} [65]:

$$R_D = V_m D\Delta P/(kTr_{cr}f_{sp}), \tag{4.15}$$

with $f_{sp} = (1 - r_{cr}/r_{ve})$; under normal conditions $r_{cr} \ll r_{ve}$ so that $f_{sp} \approx 1$ (D = diffusion coefficient, ΔP is the pressure difference between the wall of the vessel and the surface of the crystal).

In the case of cylindrical crystal in a cylindrical

vessel, eq. (4.15) is also valid with f_{cy} instead of f_{sp}; f_{cy} is given by ref. [65]: $f_{cy} = \ln(r_{ve}/r_{cr}) > 0$.

This means that R_D depends on the dimension of the diffusion field, and

$$R_{D/sp}/R_{D/cy} = \ln(r_{ve}/r_{cr})/(1 - r_{cr}/r_{ve}) > 1$$

is valid. Here $R_{D/sp}$ is the growth rate of a spherical crystal and $R_{D/cy}$ that of a cylindrical one.

For a plane crystal face ($R_{D/pl}$), eq. (4.15) is also valid, setting $f_{pl} = (r_{ve}/r_{cr} - 1)$. From this we get

$$R_{D/sp} > R_{D/cy} > R_{D/pl}.$$

Fig. 11 shows the model for an ice crystal in a diffusion field. In cases A and C (plates), $2r_{cr}$ in fig. 11 is equal to the thickness of the plate. The horizontal extent of the crystal in the figure is equal to the diameter of the (0001) face. The diffusion field on the (0001) face is a plane field and that on the $(10\bar{1}0)$ face is cylindrical. The relation

$$c/a = R_D(0001)/R_D(10\bar{1}0) = (r_{ve}/r_{cr} - 1)/\ln(r_{ve}/r_{cr}) < 1$$

is valid.

In the other cases (B and D; columns), $2r_{cr}$ in fig. 11 is equal to the diameter of the column and the length of the column is given by the horizontal extent of the crystal in the figure. The growth rate of (0001) is given by $R_{D/sp}$ (spherical field around the tip of the column) and that of $(10\bar{1}0)$ by $R_{D/cy}$ (cylindrical field around the side faces of the column). So we get

$$c/a = R_D(0001)/R_D(10\bar{1}0) = \ln(r_{ve}/r_{cr})/(1 - r_{cr}/r_{ve}) > 1.$$

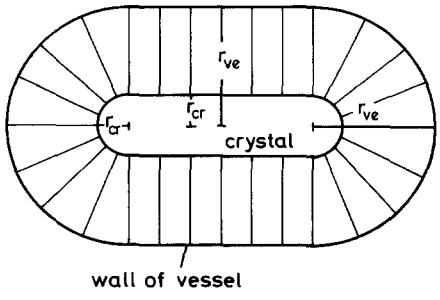

Fig. 11. Model for an ice crystal in a diffusion field.

5. Interpretation of the growth forms

The transition temperatures $T_{I/II}$ and $T_{II/III}$ of surface structure as well as growth mechanism depend on the surface orientation. We have obtained the relations

$$T_{I/II}(0001) > T_{I/II}(10\bar{1}0),$$
$$T_{II/III}(0001) > T_{II/III}(10\bar{1}0).$$

Now we assign (fig. 8):

$$T_{I/II}(0001) = -4°C, \quad T_{I/II}(10\bar{1}0) = -10°C,$$
$$T_{II/III}(0001) = -10°C, \quad T_{II/III}(10\bar{1}0) = -20°C.$$

Then we can devide the temperature region into four parts according to the combination of growth mechanism of each surface (table 2 and fig. 12).

In region A (0 to –4°C), both surfaces are covered with a quasi-liquid layer ($\vartheta > 1$) and grow by the V–QL–S mechanism.

In region B (–4 to –10°C), adhesive growth occurs on the {0001} face because of the strong eigenadsorption of water molecules ($1 > \vartheta > 0.02$), while the $\{10\bar{1}0\}$ face grows by V–QL–S mechanism.

In region C (–10 to –20°C), the singular {0001} face with little eigenadsorption ($\vartheta < 0.02$) grows by

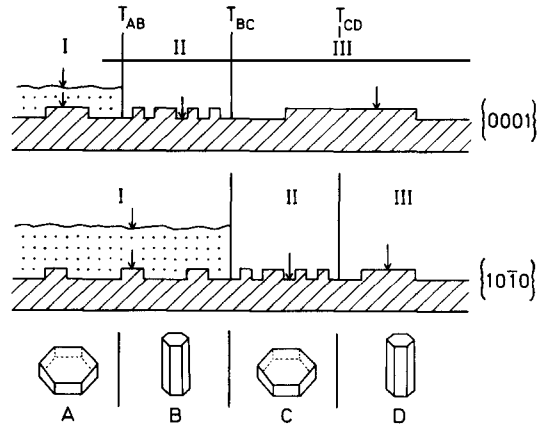

Fig. 12. Schematic representation of the combination of growth kinetics of {0001} and $\{10\bar{1}0\}$ faces depending on temperature.

Table 2
Combination of growth kinetics of 0001 and $10\bar{1}0$ faces depending on temperature

Surface	Region			
	A $0 > T > -4$°C	B $-4 > T > -10$°C	C $-10 > T > -20$°C	D $T < -20$°C
{0001}	V – QL – S mechanism ($\vartheta > 1$)	Adhesive growth ($1 > \vartheta > 0.02$)	2D nucleation growth ($\vartheta < 0.02$)	2D nucleation growth ($\vartheta < 0.02$)
$\{10\bar{1}0\}$	V – QL – S mechanism ($\vartheta > 1$)	V – QL – S mechanism ($\vartheta > 1$)	Adhesive growth ($1 > \vartheta > 0.02$)	2D nucleation growth ($\vartheta < 0.02$)

the usual two-dimensional nucleation from the vapour phase, while adhesive growth takes place on the $\{10\bar{1}0\}$ face with strong eigenadsorption.

In region C ($T < -20$°C = $T_{II/III}(10\bar{1}0)$) at small supersaturation and in region D ($T < -20$ to -35°C), both faces ($\vartheta < 0.02$) grow by the usual two-dimensional nucleation mechanism (see fig. 15).

5.1. *Growth forms determined by surface kinetics*

Fig. 13 shows the estimated growth rate $R(0001)$ (solid line), $R(10\bar{1}0)$ (broken line) and the maximum growth rate R_{max} (dot-dashed line corresponding to complete incorporation of incoming molecules into the crystals) as a function of temperature at water saturation. Here R_I is the growth rate by V–QL–S mechanism under the conditions of steady state, R_{II} the rate of adhesive growth and R_{III} the rate of two-dimensional nucleation growth. The given rates are for surface kinetics only, neglecting any effect of volume diffusion.

The numerical values used for the calculations are as follows:
(a) With regard to R_I (eqs. (4.1)–(4.3)), $\gamma_{ql}(0001) = 8.7 \times 10^{-8}$ erg/cm corresponding to 2.6×10^{-15} erg/molecule, $\gamma_{ql}(10\bar{1}0) = 6.2 \times 10^{-8}$ erg/cm corresponding to 1.8×10^{-15} erg/molecule, $f_0(0001) = 8.85 \times 10^{-16}$ cm^2, $f_0(10\bar{1}0) = 8.32 \times 10^{-16}$ cm^2, $E_d = 4.5 \times 10^{-13}$ erg/molecule, $\nu = 10^{12}$/s, $1 = 4.5 \times 10^{-8}$ cm, $m = 3.0 \times 10^{-23}$ g/molecule and $V_m = 3.0 \times 10^{-23}$ cm^3/molecule.
(b) With regard to R_{III} (eqs. (4.5)–(4.8)), $\gamma_V(0001) = 2.05 \times 10^{-6}$ erg/cm corresponding to 6.10×10^{-14} erg/molecule, $\gamma_V(10\bar{1}0) = 2.0 \times 10^{-6}$ erg/cm corresponding to 5.76×10^{-14} erg/molecule, $E_{ad} = 6.23 \times 10^{-13}$ erg/molecule, $E_{sd} = 1.73 \times 10^{-13}$ erg/molecule and $1 = 4.5 \times 10^{-8}$ cm. Here the theoretical values given by Kiefer and Hale [66] for E_{ad} and E_{sd} are used. Taking into account the entropy effect and adsorption of water molecules or other impurities at the edge, the assigned values of γ_V are smaller than the estimated values for 0°C in (III), section 4.1.

We now discuss the four growth regions in detail:
(A) In the region 0 to -4°C, both surfaces grow by V–QL–S mechanism ($\vartheta > 1$). R_I depends on the surface orientation through the rate of two-dimen-

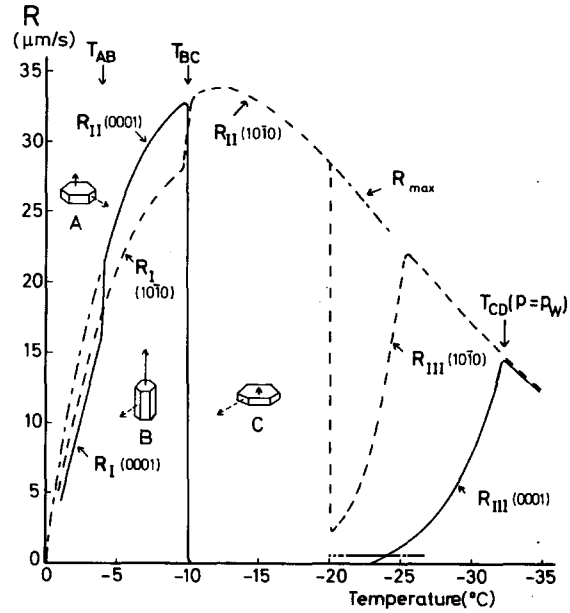

Fig. 13. The growth rates $R(0001)$ (———) and $R(10\bar{1}0)$ (– – –), and the maximum growth rate R_{max} (– · –) as a function of temperature at water saturation.

sional nucleation at the quasi-liquid/ice interface. Since the edge free energy $\gamma_{ql}(0001)$ is larger than $\gamma_{ql}(10\bar{1}0)$ the formation free energy $\Delta G^*_{2ql}(0001)$ of the critical nucleus is larger than $\Delta G^*_{2ql}(10\bar{1}0)$. Therefore the basic form of ice in the region is hexagonal plate; $c/a < 1$.

(B) Hexagonal columns ($c/a > 1$) appear in the region -4 to $-10°C$, because the adhesive growth occurs on the {0001} face which is uneven on molecular level because of strong eigenadsorption by the water molecule ($0.02 < \vartheta < 1$). The ratio of the axes c/a is, however, not as large as the observed one by Yamashita [17]. The problem is discussed in section 5.3.

(C) In the region -10 to $-20°C$, adhesive growth takes place on the $\{10\bar{1}0\}$ face with strong eigenadsorption ($0.02 < \vartheta < 1$), while a nucleation difficulty exists on the {0001} face with low eigenadsorption ($\vartheta < 0.02$). Thus, the growth form is a hexagonal plate ($c/a < 1$).

(D) Below $-20°C$, both surfaces ($\vartheta < 0.02$) grow by the usual two-dimensional nucleation. In this case, $R_{III}(10\bar{1}0)$ increases drastically with decreasing temperature because of increase in the relative supersaturation $\Delta P/P_I$, and then decreases following R_{max} ($=(P_W - P_I)\ V_m/(2\pi mkT)^{1/2}$), as the step velocity decreases because of the step–step interaction at such large $(P_W - P_I)/P_I$. On the other hand, $R_{III}(0001)$ begins to increase at lower temperature ($-23°C$) than $R_{III}(10\bar{1}0)$ because of the larger formation free energy $\Delta G^*_{2V}(0001)$ of the two-dimensional critical nucleus and reaches $R_{III}(10\bar{1}0)$ at $-32°C$ (fig. 13). Therefore, $c/a < 1$ in the region -20 to $-32°C$ and $c/a \approx 1$ below $-32°C$ at water saturation. The columnar crystals at temperatures below $-20°C$/ $-35°C$ cannot be understood as long as the growth rate is determined only by surface kinetics. They are due to the shape effect of the diffusion field discussed in section 4.2.

5.2. *Appearance of columnar crystals in region D ($T < -20°C$)*

It has been shown in section 4.2 that the incoming flux of water molecules to {0001} faces is much larger than that to $\{10\bar{1}0\}$ faces because of the effect of the diffusion field surrounding a columnar crystal ($c/a > 1$). This tendency would be also expected,

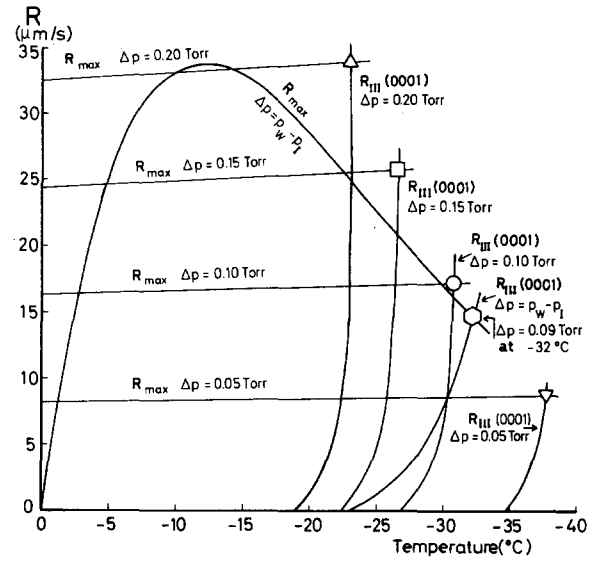

Fig. 14. $R_{III}(0001)$ and R_{max} at constant ΔP and at water saturation $\Delta P = P_W - P_I$ as a function of temperature.

even if $c/a \approx 1$, since the water molecules impinge to the {0001} face approximately from three-dimensional directions and to the $\{10\bar{1}0\}$ faces from two directions. Therefore the {0001} face is preferred to $\{10\bar{1}0\}$. Accordingly, if the surface kinetics $R_{III}(0001)$ are equal to $R_{III}(10\bar{1}0)$, one would

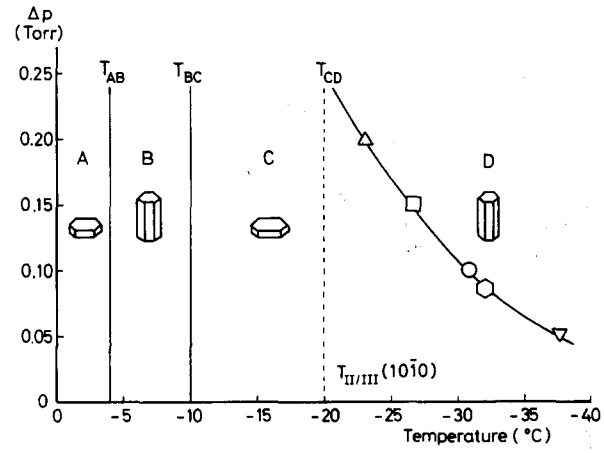

Fig. 15. Theoretical diagram showing the relation between basic forms of ice crystals and growth conditions. The ΔP dependence of the third conversion temperature $T_{CD}(\Delta P)$ is obtained from fig. 14.

expect $c/a \approx 1$, but c/a becomes gradually larger than 1 due to this diffusion effect. For example, $R_{III}(0001) = R_{III}(10\bar{1}0) = R_{max}$ at $-32°C$ and $\Delta P = P_W - P_I = 0.07$ Torr. The columnar crystals would appear at $T < -32°C$ and $\Delta P = 0.09$ Torr or at $T = -32°C$ and $\Delta P > 0.07$ Torr. Therefore the third transition temperature $T_{CD}(\Delta P)$ from plates to columns depends on ΔP.

We can obtain T_{CD} as a function of ΔP as the locus of points in the ΔP–T plane where $R_{III}(0001)$ agrees with R_{max}, because $R_{III}(0001) = R_{max}$, which means that $R_{III}(0001) = R_{III}(10\bar{1}0)$. Fig. 14 shows $R_{III}(0001)$ and R_{max} at constant ΔP or at water saturation. Fig. 15 is a theoretical diagram showing the relation between basic growth forms of ice crystals from vapour phase and growth conditions.

5.3. *Influence of diffusion on columnar crystals in region B (−4 to −10°C)*

As mentioned in section 5.1, the estimated ratio c/a does not differ from unity as much as the observed ratio. As the growth rate is fairly large in region B (fig. 13), the diffusion of the water vapour plays a great roll as a rate determining process (see section 4.2).

If we use eqs. (4.15) and the equation with f_{cy}, we can estimate the ratio c/a $(=\ln(r_{ve}/r_{cr})/(1 - r_{cr}/r_{ve}))$ under consideration of the diffusion. Table 3 shows the ratio c/a as a function of r_{ve}/r_{cr} and suggests that diffusion field makes the columnar crystals formed by surface kinetics more marked ($c/a \gg 1$).

Since the number of the falling ice crystals in Yamashita's experiments is about $7 \times 10^3/m^3$, one half of the mean distance r_{ve} between crystals is about 2.5 cm. In order to estimate $R(0001)$ and $R(10\bar{1}0)$ using eqs. (4.15) and the equation with f_{cy}, we assign $r_{ve} = 2.5$ cm, $r_{cr} = 5 \times 10^{-4}$ cm, $V_m = 3.29 \times 10^{-23}$ cm³/molecule, $D = 0.2$ cm²/s, $T = 267.15$ K (=−6°C) and $\Delta P = P_W - P_I = 0.17$ Torr. We have obtained

$$R(0001) = 0.81\ \mu m/s, \quad R(10\bar{1}0) = 0.09\ \mu m/s.$$

The corresponding values using the measured length of c and a axis at 200 s after seeding by Yamashita [17] (fig. 2) are

$$R_{exp}(0001) = 0.43\ \mu m/s, \quad R_{exp}(10\bar{1}0) = 0.09\ \mu m/s.$$

The calculated values are in fairly reasonable agreement with R_{exp}.

Table 3
The ratio c/a under consideration of diffusion depending on r_{ve}/r_{cr}

r_{ve}/r_{cr}	c/a
10	2.56
10^2	4.65
10^3	6.91
10^4	9.21

5.4. *Influence of diffusion to plate-like crystals in region A (0 to −4°C) and C (−10 to −20°C/−35°C)*

At temperatures between 0 and −4°C, the habit determined by surface kinetics is hexagonal plate-like ($c/a < 1$). The estimated value of c/a (fig. 13) is, however, not as small as that observed by Yamashita [17] (fig. 2). As mentioned in section 4.2, the diffusion field would make the plate more thinner.

On the other hand, the growth of {0001} faces with low eigenadsorption in region C is strongly restrained by the nucleation difficulty. Therefore, the admolecules which impinged on {0001} faces within $\bar{x}_s$ from the edges between {0001} and $\{10\bar{1}0\}$ faces migrate on the surface towards $\{10\bar{1}0\}$ faces where molecules can be easily incorporated into the crystal, and contribute to the growth of $\{10\bar{1}0\}$ faces. According to a rough estimation, $R(10\bar{1}0)$ can be expressed by

$$R(10\bar{1}0) = \frac{V_m \Delta P}{(d/2)} \left[\frac{D}{kT \ln[r_{ve}/(d/2)]} + \frac{\bar{x}_s}{(2\pi mkT)^{1/2}} \right]. \tag{5.1}$$

Here d is the thickness of the plate. The first term corresponds to the direct incoming molecules to $\{10\bar{1}0\}$ faces from the vapour by diffusion and the second term to the surface diffusion on {0001} faces towards $\{10\bar{1}0\}$ faces.

If we use $D = 0.2$ cm²/s, $d = 5 \times 10^{-4}$ cm, $\bar{x}_s = 5001^* = 2.25 \times 10^{-5}$ cm, and $\Delta P = 0.2$ Torr at

* If the theoretical values for E_{ad} and E_{sd} (see (b) in section 5.1) are inserted in eq. (4.8), the given value for $\bar{x}_s$ is obtained.

$-14°C$, we obtain

$R(10\bar{1}0) = 3.0\ \mu m/s.$

The contribution of the surface diffusion to $R(10\bar{1}0)$ in eq. (5.1) is 15 times larger than that of the volume diffusion. The corresponding $R_{exp}(10\bar{1}0)$ in Yamashita's experiments (fig. 2) is

$R_{exp}(10\bar{1}0) = 1.4\ \mu m/s.$

6. Discussion

6.1. Growth forms

In the former section, we have interpreted three conversion temperatures of habit changes of ice crystals growing from the vapour phase. The first conversion temperature, T_{AB} (= $-4°C$), is the temperature $T_{I/II}(0001)$ where the V–QL–S mechanism of {0001} faces ($\vartheta > 1$) changes into the adhesive growth due to the strong eigenadsorption ($1 > \vartheta > 0.02$). The second, T_{BC} (= $-10°C$), is the transition temperature $T_{I/II}(10\bar{1}0)$ from V–QL–S mechanism of $\{10\bar{1}0\}$ faces to the adhesive growth and $T_{II/III}$ of $\{000\bar{1}\}$ faces from adhesive growth to the normal two-dimensional nucleation growth ($\vartheta < 0.02$). $T_{CD}(\Delta P)$ is the temperature where the two-dimensional nucleation growth rate of {0001} faces reaches that of $\{10\bar{1}0\}$ faces and exceeds it due to diffusion effects.

The following features of the conversion temperatures should be noticed. Since T_{AB} and T_{BC} are concerned with changes in surface structure depending on temperature, they are independent on supersaturation. Therefore, the first and second conversions of basic habits occur within temperature intervals of less than 1 K (Kobayashi [7]), even though the absolute values of T_{AB} and T_{BC} are a little different according to experiments, show some scatter between different experimentators: e.g. $T_{AB} = -4°C$ (Aufm Kampe et al. [4], Mason [5], Kobayashi [6,7] and Yamashita [17]), and $-3°C$ (Hallett and Mason [8]), $T_{BC} = -10°C$ (Nakaya [3], Mason [5] and Kobayashi [6,7]), $-9°C$ (Aufm Kampe et al. [4]), and $-8°C$ (Hallett et al. [8] and Yamashita [17]). The difference is probably caused by errors in the measurements of the surface temperature of the crystal or different contamination of the surface or simply different judgement of when c/a equals unity. In fact, one always gets a c/a distribution with a more or less pronounced maximum.

On the other hand, $T_{CD}(\Delta P)$ depends on the supersaturation ΔP. The nucleation rate J increases abruptly with increasing relative supersaturation $\Delta P/P_I$ (see eqs. (4.6), (4.9) and (4.10)). Since P_I decreases with falling temperature, $R_{III}(0001)$ reaches $R_{III}(10\bar{1}0)$ at smaller absolute supersaturation with decreasing temperature. Therefore, $T_{CD}(\Delta P)$ falls with decreasing ΔP. Recently hexagonal plates have been observed [10–12] at temperatures below $-30°C$ and low supersaturation. Anderson et al. [11] reported that the hexagonal column was dominant for the habit of ice crystals only at higher supersaturation (e.g. $\Delta P/P_I > 25\%$ at $-38°C$). Gonda [12] found that small crystals ($<30\ \mu m$) grown in free fall in helium or argon gas at $-30°C$ and about 4% supersaturation, and at $-44°C$ and near ice saturation, were almost plates. Kikuchi and Hogan [10] observed diamond dust type ice crystals at around $-35°C$ air temperature and supersaturations less than 40% at Amundsen Scott South Pole Station. Columnar crystals prevailed, but occasionally more than half of the crystals were plate-like. These results are consistent with our theoretical prediction about $T_{CD}(\Delta P)$. The precise measurement of the $T_{CD}(\Delta P)$ curve is desirable. If ice crystals grow in water vapour without air and any other gases, the rate of growth is not determined by the diffusion process but only by surface kinetics. Thus, columnar crystals would never appear at temperatures below $-20°C$, even if ΔP is larger than the value given by $T_{CD}(\Delta P)$ curve.

In sections 4.2, 5.2, 5.3 and 5.4, it has been shown that the observed extremely long ($c/a \gg 1$) columnar crystals were caused by the spherical volume diffusion field near the {0001} faces and the cylindrical one near the $\{10\bar{1}0\}$ faces, and thin plate-like crystals by the plane field near the {0001} faces and the cylindrical one near the $\{10\bar{1}0\}$ faces. Gonda and Komabayashi [22] and Gonda [23] showed experimentally that the extreme ratio of axes c/a approaches unity as D increases (fig. 4). The results clearly support the effect of diffusion discussed in this paper.

6.2. Growth kinetics

In order to interpret the change in basic habits of ice crystals, we discussed the dependence on temperature of three kinds of surface kinetics of growth, i.e. (I) V–QL–S mechanism, (II) Adhesive Growth of the surface with strong eigenadsorption, and (III) the usual Two-Dimensional Nucleation Growth of the surface with low eigenadsorption. On the other hand, the supersaturation dependence of each surface kinetics at constant temperature is also of interest.

The steady state growth rate in the case of V–QL–S mechanism is obtained from the condition (see fig. 10):

$$R_{Ia}(\delta_{st}(T), \Delta P) = R_{Ib}(\delta_{st}(T)).$$

Therefore, $R_I(T, \Delta P)$ does not show the exponential increase with increasing supersaturation, even if the two-dimensional nucleation at quasi-liquid/ice interface contributes to R_{Ib}. Fig. 16 shows the ΔP dependence of the calculated growth rate $R_I(10\bar{1}0)$ (solid line), the measured one by Lamb and Scott [27] (dotted line), and R_{max} which is given by eq. (4.4) and corresponds to R_{Ia} for $\delta = \delta_{eq}$. $R_I(10\bar{1}0)$ shows at first a quadratic and then a linear trend as found in experiments.

The edge free energy γ_{ql} of a two-dimensional nucleus at quasi-liquid/ice interface is so much

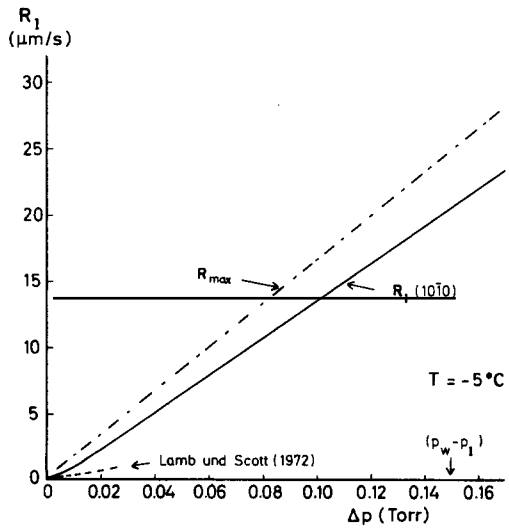

Fig. 16. $R_I(10\bar{1}0)$ as a function of ΔP in case of V–QL–S mechanism at –5° C.

smaller than that on the surface with low eigenadsorption at low temperature (γ_V), that such a large growth rate of 0.1 μm/s at a relative supersaturation below 1% (in table 1) is possible.

Incidentally, the stationary growth rate R_I in case of a V–QL–S mechanism does not exist for too high temperatures at constant supersaturation and for too large supersaturations at constant temperature (Kuroda [57]). It should also be noticed that R_I is independent of the relation of the equilibrium vapour pressure of a quasi-liquid layer $P(\delta)$ [57].

Beaglehole et al. [54] found by means of ellipsometry that $T_{I/II}(10\bar{1}0) = -10°C < T_{I/II}(0001)$. The result is in good agreement with the expected anisotropy in section 3.

The rate of adhesive growth R_{II} is proportional to ΔP (eq. (4.4)), while the two-dimensional nucleation growth of the surface with little eigenadsorption is characterized by the exponential increase of R_{III} with increasing $\Delta P/P_I$. The dominant surface kinetics depending on temperature can be determined experimentally by the measurement of the supersaturation dependence of the growth rate at various temperatures. Lamb and Scott [27] carried out such investigations in a limited temperature region. For example, the growth rate of $\{10\bar{1}0\}$ faces at –16.8°C was proportional to ΔP. The result confirms the adhesive growth of $\{10\bar{1}0\}$ faces with strong eigenadsorption at temperatures between $T_{I/II}(10\bar{1}0) = -10°C$ and $T_{II/III}(10\bar{1}0) = -20°C$. The peak in the growth rate of the c axis at –6°C and that of the a axis at –15°C in fig. 2 after Yamashita are caused by adhesive growth of {0001} and $\{10\bar{1}0\}$ faces, respectively (cp. fig. 13). Precise measurements of the ΔP dependence of the growth rates of both {0001} and $\{10\bar{1}0\}$ faces in a wide temperature range are now being prepared in the Institute of Physical Chemistry at the Technical University Braunschweig.

We have obtained the edge free energy $\gamma_V(0001)$ and $\gamma_V(10\bar{1}0)$ using the Stranski–Kaischev method, i.e.

$$\gamma_V^{th}(0001) = 4.7 \times 10^{-6} \text{ erg/cm},$$
$$\gamma_V^{th}(10\bar{1}0) = 3.7 \times 10^{-6} \text{ erg/cm}.$$

The calculation corresponds to the edge free energy at 0 K. It decreases with temperature because of the increase in entropy due to roughening of the edge. The temperature dependence of γ has been investi-

gated by Franke [67] and Franke and Lacmann [68] using Monte-Carlo simulation. The adsorption of water molecules or other impurities at the edge reduces the value of γ_V. Therefore, the smaller values are used for $\gamma_V(0001)$ and $\gamma_V(10\bar{1}0)$ in calculations of R_{III}, i.e.

$\gamma_V(0001) = 2.05 \times 10^{-6}$ erg/cm,
$\gamma_V(10\bar{1}0) = 2.0 \times 10^{-6}$ erg/cm.

In the temperature range -10 to -20°C, the growth of {0001} face with low eigenadsorption is extremely restrained by the nucleation difficulties (fig. 13). In the experiments by Anderson et al. [11] the {0001} face hardly grows in this temperature range and at water saturation.

The molecules impinging to {0001} faces diffuse on the surface towards $\{10\bar{1}0\}$ faces where adhesive growth takes place, and contribute to the growth of $\{10\bar{1}0\}$ faces. The contribution of the surface diffusion to the growth rate is about 15 times larger than that of the direct volume diffusion at -14°C (section 5.4). The same effect of the surface diffusion was found by Dittmar et al. [69] in case of growth of potassium whisker. The growth rate in the direction of its length was much larger than the expected rate according to the direct incoming flux from the vapour to the top of the whisker. They estimated the mean surface diffusion distance $\bar{x}_s$ on the side {011} faces from the measured axial growth rate. In the same manner, the $\bar{x}_s$ on the {0001} faces of ice crystal is to be determined by the measurement of $R(10\bar{1}0)$ in the temperature region (-10 to -20°C and by eq. (5.1). Eq. (5.1) shows that $R(10\bar{1}0)$ is inversely proportional to the thickness of the plate-like crystal if the first term (volume diffusion) is negligible against the second term (surface diffusion). This relation has been found experimentally by McKnight and Hallett [19].

In this paper we assume that the ice crystals growing from the vapour are dislocation free. McKnight and Hallett [19] have confirmed, actually using X-ray topography, that the plate-like ice crystals were often free from dislocations.

Acknowledgement

This work was carried out during one of the authors' (T.K.) stay at the Technische Universität Braunschweig. He wishes to express his gratitude to Konrad-Adenauer-Stiftung for the financial support. We would like to thank the Fonds der Chemischen Industrie for supporting this work and Dr. W. Beckmann for the critical reading of the manuscript.

References

[1] U. Nakaya, I. Sato and Y. Sekido, J. Fac. Sci. Hokkaido Univ., Ser. II, 2 (1938) 1;
U. Nakaya, Y. Toda and S. Maruyama, J. Fac. Sci. Hokkaido Univ., Ser. II, 2 (1938) 1.
[2] M. Hanajima, Low. Temp. Sci. A1 (1944) 53; A2 (1949) 23.
[3] U. Nakaya, in: Compendium of Meteorology (Am. Meteorol. Soc., Boston, MA, 1951) p. 207;
U. Nakaya, Snow Crystals – Natural and Artificial (Harvard Univ. Press, 1954).
[4] H.J. Aufm Kampe, H.K. Weickmann and J.J. Kelly, J. Metals 8 (1951) 168.
[5] B.J. Mason, Quart. J. Roy. Meteorol. Soc. 79 (1953) 104.
[6] T. Kobayashi, J. Meteorol. Soc. Japan 75th Ann. Vol. (1957) 38; J. Meteorol. Soc. Japan 36 (1958) 193.
[7] T. Kobayashi, Phil. Mag. 6 (1961) 1363.
[8] J. Hallett and B.J. Mason, Proc. Roy. Soc. (London) A247 (1958) 440.
[9] B.J. Mason, G.W. Bryant and A.P. Van den Heuvel, Phil. Mag. 8 (1963) 505.
[10] K. Kikuchi and A.W. Hogan, J. Meteorol. Soc. Japan 57 (1979) 180.
[11] B.J. Anderson, V. Keller, C. McKnight and J. Hallett, in: Proc. Intern. Conf. on Cloud Physics, Ed. H.K. Weickmann (Am. Meteorol. Soc., Boston, MA, 1976) p. 97.
[12] T. Gonda, J. Meteorol. Soc. Japan 55 (1977) 142.
[13] F.C. Frank, J. Crystal Growth 24/25 (1974) 3.
[14] A.A. Chernov, J. Crystal Growth 24/25 (1974) 11.
[15] T. Kuroda, T. Irisawa and A. Ookawa, J. Crystal Growth 42 (1977) 41.
[16] R. Lacmann and I.N. Stranski, J. Crystal Growth 13/14 (1972) 236.
[17] A. Yamashita, Kisho Kenkyu Note, Meteorol Soc. Japan 123 (1974) 813.
[18] B.F. Ryan, E.R. Wishart and D.E. Shaw, J. Atmospheric Sci. 33 (1976) 842.
[19] C.V. McKnight and J. Hallett, J. Glaciology 21 (1978) 397.
[20] V.W. Keller, C.V. McKnight and J. Hallett, J. Crystal Growth 49 (1980) 458.
[21] K. Isono, M. Komabayashi and A. Ono, J. Meteorol. Soc. Japan 35 (1957) 17.
[22] T. Gonda and M. Komabayashi, J. Meteorol. Soc. Japan 48 (1970) 440; 49 (1971) 32.
[23] T. Gonda, J. Meteorol. Soc. Japan 54 (1976) 233; J. Crystal Growth 49 (1980) 173.

[24] J. Hallett, Phil. Mag. 6 (1961) 1073.
[25] T. Kobayashi, in: Physics of Snow and Ice, Vol. 1 (Hokkaido Univ., Sapporo, 1967) p. 95.
[26] D. Lamb and P.V. Hobbs, J. Atmospheric Sci. 28 (1971) 1506.
[27] D. Lamb and W.D. Scott, J. Crystal Growth 12 (1972) 21.
[28] M. Volmer and W. Schultze, Z. Physik. Chem. 156 (1931) 1.
[29] R.S. Bradley and T. Drury, Trans. Faraday Soc. 55 (1959) 1848.
[30] B. Honigmann and H. Heyer, Z. Elektrochem. 61 (1957) 74.
[31] R.L. Parker and L.M. Kushner, J. Chem. Phys. 35 (1961) 1345.
[32] S.A. Kitchener and R.F. Strickland-Constable, Proc. Roy. Soc. (London) A245 (1958) 93.
[33] M. Faraday, Lecture at Royal Institution, London, 7 June 1850, Phil. Mag. (4th Ser.) 17 (1859) 162; Proc. Roy. Soc. (London) 10 (1860) 440; Researches in Chemistry and Physics (Bell, London, 1933) p. 373.
[34] W.A. Weyl, J. Colloid Sci. 6 (1951) 389.
[35] N.H. Fletcher, Phil. Mag. 7 (1962) 255; 18 (1968) 1287;
N.H. Fletcher, in: Physics and Chemistry of Ice, Eds. E. Whalley et al. (Royal Soc. Canada, Ottawa, 1973).
[36] U.Nakaya and A. Matsumoto, J. Colloid Sci. 9 (1954) 41.
[37] D.C. Jensen MS Thesis, Pennsylvania State Univ., State College, Pennsylvania (1956).
[38] C.L. Hosler, D.C. Jensen and L. Goldshlak, J. Meteorol, 14 (1957) 415.
[39] H.H.G. Jellinek, J. Colloid Sci. 14 (1959) 268; Can. J. Phys. 40 (1962) 1294; J. Colloid Interface Sci. 25 (1967) 192;
H.H.G. Jellinek, in: Water and Aqueous Solutions, Ed. R.A. Horne (Wiley–Interscience, New York, 1972).
[40] S. Mantovani and S. Valeri, Phil. Mag. A37 (1978) 17.
[41] R.R. Gilpin, J. Colloid Interface Sci. 68 (1978) 235.
[42] C. Jaccard, Z. Angew. Math. Physik 17 (1966) 657; Physics C. Jaccard, in: Physics of Snow and Ice, Vol. 1 (Hokkaido Univ., Sapporo, 1967) p. 173.
[43] M. Kopp, Z. Angew. Math. Physik 13 (1962) 431.
[44] B. Bullemer and N. Riel, Solid State Commun. 4 (1966) 447.
[45] N. Maeno and H. Nishimura, J. Glaciol. 21 (1978) 193.
[46] A.W. Adamson, I.M. Dormant and M. Orem, J. Colloid Interface Sci. 25 (1967) 206.
[47] M.W. Orem and W.A. Adamson, J. Colloid Interface Sci. 31 (1969) 278.
[48] V.I. Kvlividze, V.F. Kiselev and I.A. Ushakova, Dokl. Akad. Nauk SSSR 191 (1970) 1088 (engl. translation p. 307).
[49] V.L. Kvlividze, V.F. Kiselev, A.B. Kurzaev and L.A. Ushakova, Surface Sci. 44 (1974) 60.
[50] D. Nason and N.H. Fletcher, J. Chem. Phys. 62 (1975) 4444.
[51] E. Mazzega, U. del Pennino, A. Loria and S. Mantovani, J. Chem. Phys. 64 (1976) 1028.
[52] I. Golecki and C. Jaccard, Phys. Letters 63A (1977) 374.
[53] S. Valeri and S. Mantovani, J. Chem. Phys. 69 (1978) 5207.
[54] D. Beaglehole and D. Nason, Surface Sci. 96 (1980) 357.
[55] D. Lamb and W.D. Scott, J. Atmospheric Sci. 31 (1974) 570.
[56] R. Lacmann, Z. Physik. Chem. (NF) 104 (1977) 1.
[57] T. Kuroda, Dissertation, Technical University Braunschweig (1979).
[58] E. Ruckenstein, J. Crystal Growth 47 (1979) 666.
[59] S.C. Hardy, Phil. Mag. 35 (1977) 471.
[60] F.W. Schulze and H. Cammenga, Ber. Bunsenges. Physik. Chem. 84 (1980) 163.
[61] W.B. Hillig, Acta Met. 14 (1966) 1968.
[62] W.B. Hillig, in: Growth and Perfection of Crystals, ed. R. Doremus, John Wiley (1958), 350.
[63] S.W.H. de Haan, V.J.A. Meeussen, B.P. Veltman, P. Bennema, C. van Leeuwen and G.H. Gilmer, J. Crystal Growth 24/25 (1974) 491.
[64] R. Lacmann, Neues Jahrb. Mineral. Abh. 122 (1974) 36.
[65] J. Crauk, The Mathematics of Diffusion (Clarendon, Oxford, 1957).
[66] J. Kiefer and B.N. Hale, J. Chem. Phys. 7 (1977) 3260.
[67] H. Franke, Dissertation, Technical University Braunschweig (1978).
[68] H. Franke and R. Lacmann, Phys. Status Solid, (a) 55 (1979) 415; 60 (1980) 475.
[69] W. Dittmar and K. Neumann, Z. Elektrochem. 64 (1960) 297;
W. Dittmar and S. Mennicke, Z. Physik. Chem. (NF) 71 (1970) 255.